Building Structure-Property Relationships of Cycloalkanes in Support of Their Use in Sustainable Aviation Fuels

Alexander Landera[1]*, Ray P. Bambha[1], Naijia Hao[2], Sai Puneet Desai[2], Cameron M. Moore[2], Andrew D. Sutton[2†] and Anthe George[1]

[1]Sandia National Laboratories, Livermore, CA, United States, [2]Los Alamos National Laboratory, Los Alamos, NM, United States

In 2018 13.7 EJ of fuel were consumed by the global commercial aviation industry. Worldwide, demand will increase into the foreseeable future. Developing Sustainable Aviation Fuels (SAFs), with decreased CO_2 and soot emissions, will be pivotal to the on-going mitigation efforts against global warming. Minimizing aromatics in aviation fuel is desirable because of the high propensity of aromatics to produce soot during combustion. Because aromatics cause o-rings to swell, they are important for maintaining engine seals, and must be present in at least 8 vol% under ASTM-D7566. Recently, cycloalkanes have been shown to exhibit some o-ring swelling behavior, possibly making them an attractive substitute to decrease the aromatic content of aviation fuel. Cycloalkanes must meet specifications for a number of other physical properties to be compatible with jet fuel, and these properties can vary greatly with the cycloalkane chemical structure, making their selection difficult. Building a database of structure-property relationships (SPR) for cycloalkanes greatly facilitates their furthered inclusion into aviation fuels. The work presented in this paper develops SPRs by building a data set that includes physical properties important to the aviation industry. The physical properties considered are energy density, specific energy, melting point, density, flashpoint, the Hansen solubility parameter, and the yield sooting index (YSI). Further, our data set includes cycloalkanes drawn from the following structural groups: fused cycloalkanes, n-alkylcycloalkanes, branched cycloalkanes, multiple substituted cycloalkanes, and cycloalkanes with different ring sizes. In addition, a select number of cycloalkanes are blended into Jet-A fuel (POSF-10325) at 10 and 30 wt%. Comparison of neat and blended physical properties are presented. One major finding is that ring expanded systems, those with more than six carbons, have excellent potential for inclusion in SAFs. Our data also indicate that polysubstituted cycloalkanes have higher YSI values.

Keywords: structure-property relationship, jet fuel, cycloalkane, o-ring, physical properties

1 INTRODUCTION

In 2012 the aviation sector accounted for 11% of the world's transportation energy (International Energy Outlook, 2016). By 2040 global energy demand for aviation fuel is forecast to increase by 10.6 EJ. This increase is concerning because the continued combustion of petroleum fuel will emit more CO_2 into the atmosphere and with it comes larger effects from global warming. The fifth Assessment Report of the Intergovernmental Panel on Climate Change (IPCC), published in 2014, concluded that in 2010 aviation accounted for 10.62% of the global CO_2 emitted within the transportation sector (Sims et al., 2014). Although, CO_2 emissions from road transportation is increasing at a faster absolute pace, when viewed by percent CO_2 change, gains in the aviation sector are faster. Further, unlike other forms of travel, such as cars and trucks, there is no foreseeable path to electrify the aviation sector. Therefore, mitigation efforts are necessary to decarbonize the aviation industry. Sustainable Aviation Fuels (SAFs) are produced from renewable feedstocks and offer the potential of a lower carbon intensive alternative to current petroleum refined jet fuels. There are currently seven approved SAFs, which are approved as blends of 50% or lower by volume with conventional jet fuel: Fischer-Tropsch Synthetic Paraffinic Kerosene (FT-SPK), Hydroprocessed Esters and Fatty Acids Synthetic Paraffinic Kerosene (HEFA-SPK), Hydroprocessed Fermented Sugars to Synthetic Isoparaffins (HES-SIP), Fischer-Tropsch Synthetic Paraffinic Kerosene with Aromatics (FT-SPK/A), Alcohol to Jet Synthetic Paraffinic Kerosene (ATJ-SPK), Catalytic Hydrothermolysis Synthesized Kerosene (CH-SK), and Hydrocarbon-Hydroprocessed Esters and Fatty Acids (HC-HEFA-SPK) (ASTM D7566, 2015). SAF developed biofuels are attractive because they can significantly reduce CO_2 emissions over their life cycle and also decrease sooting and radiative forcing through the inhibition of contrail formation (Yang et al., 2019). A recent review highlighted these reductions by pointing out that many biojet fuels show large decreases in particulate matter ranging from 25 to 95% over conventional jet fuels (Yang et al., 2019).

Whilst SAFs can enable soot reduction from aromatics, a minimum quantity of aromatics are required in aviation fuel, according to ASTM-D7566, to ensure sufficient seal swelling in the aircraft and fuel circulation systems (ASTM D7566, 2015). The degree of fuel swelling is dependent on the material o-rings are made from and the type of aromatic molecules present in the fuel. Previous work with nitrile rubber shows that fuel swelling increases with the hydrogen bonding character, and the polarity of an aromatic molecule (Graham et al., 2006). In addition, lower molecular weight aromatics were found to increase o-ring swelling. Similar results were shown in acrylonitrile- butadiene o-rings, in which smaller, less hindered, aromatics were observed to cause o-ring swelling (Romanczyk et al., 2019). Cycloalkanes have also been shown to induce some o-ring swelling (Balster et al., 2008; Kosir et al., 2020). Recent research shows that cycloalkanes must be present in significant amounts to achieve a comparable amount of o-ring swelling to Jet-A. A recent study by Boeing shows that when "active cycloparaffins" are present in

TABLE 1 | Jet-A constraints and Median Jet-A values for the physical properties considered in this work. Jet-A constraints come from ASTM D7566, and median values come from the Petroleum Quality Information System, and consists of 770 data points.

Physical property	Constraint	Median value
Specific Energy, MJ/kg	>42.8	43.20
Energy Density, MJ/L	***	34.90
Density at 15°C, kg/m^3	775–840	810
Flashpoint, °C	>38C	46.39
Melting point, °C	<−40	−49.43

SPK fuels at 30 vol% an o-ring swelling behavior similar to a low aromatic Jet-A fuel is achieved (Graham et al., 2011). Other work has shown that at least 60% decalin was needed in order to swell nitrile o-rings to a level comparable to Jet A-1 (Liu and Wilson, 2012). It is apparent that, with respect to cycloalkanes, the type and amount of cycloalkanes is a crucial component in determining the degree of o-ring swelling observed. Jet-A (POSF-10325) is composed of on average 32 wt% total cycloalkanes (mono and bicyclic alkanes) (Holladay et al., 2020). If cycloalkanes are blended into Jet-A at 10 or 30 wt%, the cycloalkane content of a typical fuel increases from 32 wt% to 40 or 52 wt%, respectively. Depending on which cycloalkane is blended, this may yield sufficient o-ring swelling in at least some o-ring materials used in aviation. In addition to o-ring swelling behavior, SAFs must meet a number of criteria for physical properties. These criteria are part of the ASTM-D7566 testing protocol and are provided in **Table 1** (ASTM D7566, 2015). These specifications are based on operability, safety, and performance of the aircraft. Currently, information on the physical properties of a large range of cycloalkanes is limited. Moreover, the data that are available is distributed across a wide expanse of literature covering a large number of research areas. Researchers aiming to convert feedstocks into SAFs must have reliable estimates or measurements of the physical properties of cycloalkanes so that they can target fuels that meet specification.

The chemical space occupied by cycloalkanes is large and experimental measurements of even a small fraction of this space is not tractable. Computational models have been shown to be fast, efficient, and accurate and can therefore cover a larger portion of this chemical space. Supplementing experimental measurements with predictions can enable the development of Structure-Property Relationships (SPRs) and trends deduced from these SPRs will allow researchers to better select new SAF targets for production. This paper attempts to deduce SPRs by predicting relevant physical properties. Data are obtained from many different sources and are supplemented with estimates from computational models. The physical properties considered in this paper are freezing point, physical density, specific energy, energy density, flashpoint, and Hansen solubility parameter (HSP). These are shown in **Table 1** along with the required values for a reference aviation fuel, Jet-A (As per ASTM D7566) (ASTM D7566, 2015). Cycloalkanes are split into different groups based on their structural features and the influence of those structural features on the physical properties are used to infer SPRs. In addition, data of blends with some

promising cycloalkanes are shown and discussed. When in this paper, minimums and maximums of Jet-A properties are referenced they are always in regards to the specifications of Jet-A properties as laid out in ASTM-D1655 (ASTM D1655, 2019). In addition, when reference is made to median Jet-A specific energy and energy density values these values are taken from 770 PQIS (Petroleum Quality Information System) data points (Defense Technical Information Center, 2013).

2 MATERIALS AND METHODS

When available, data from National Institute of Standards and Technology, NIST, or experimental data from the literature were used (Kazakov et al., 2002; Acree and Chickos, 2011; Bradley and Andrew, 2014). When data from the literature are used it is cited in the appropriate section, where it is used. However, many values used in generating SPRs are derived from computational models. These models are described below. The accuracy of each computational model is described in **Section 3**.

2.1 SAFT-γ-Mie

The SAFT-γ-Mie EoS is used to predict physical properties when no experimental or other more accurate method is unavailable. The SAFT-γ-Mie EoS attempts to accurately model the Helmhotz free energy (A), by decomposing A into different parts. A is obtained through the following equation:

$$A = A^{ideal} + A^{mono} + A^{chain} + A^{assoc} \qquad (1)$$

where A^{ideal} is the Helmholtz free energy obtained through the ideal gas law, A^{mono} is the residual accounting for monomeric Mie segment interactions, A^{chain} is the residual accounting for molecule formation, and A^{assoc} is a term that accounts for association interactions. With each additional term in the expansion, a more realistic chemistry is obtained, and a more realistic representation of A is realized. An exact expression for A^{ideal} is known, and the other terms can be determined through group contribution theory perturbation theory or Wertheim's first-order perturbation theory (TPT1) (Barker and Henderson, 1967; Wertheim, 1984a; Wertheim, 1984b; Wertheim, 1986a; Wertheim, 1986b). Once A is known, physical properties can be determined using simple partial derivative relations i.e., such as Maxwell's equations.

2.2 Specific Energy, Energy Density, and Density

Using the coefficients of a balanced combustion reaction, the enthalpy of combustion can be calculated using a quantum chemistry composite method, such as, CBS-QB3 method (Montgomery et al., 2000). The energy required to vaporize the cycloalkane is accounted for by using the standard heat of vaporization, which is calculated using the SAFT-γ-Mie Equation of State (EoS). The enthalpy of combustion, once calculated, is then converted to the specific energy by using the molecular weight as a conversion factor. The energy density is calculated by multiplying the Specific Energy by the density of the target molecule at 25°C. The SAFT-γ-Mie EoS is used to calculate densities, and a description of the SAFT-γ-Mie EoS is provided above.

2.3 Flashpoint

The flashpoint of a pure molecule is calculated using an empirical equation that has been shown to be accurate for a wide range of compounds (Catoire and Naudet, 2004). The inputs to the flashpoint equation, **Eq. 2**, are the number of carbon atoms, the normal boiling point, and the standard heat of vaporization (Catoire and Naudet, 2004). This equation is accurate for flashpoints that are between −100 and 200°C, normal boiling points (NBP) that are between 250 and 650 K, standard enthalpies of vaporization ($\triangle H_{vap}$ (298.15)) between 20 and 110 kJ mol^{-1}, and number of carbon atoms (C_{num}) between 1 and 21. NBP are obtained from the literature, when possible, but, if not possible, are calculated using the SAFT-γ-Mie EoS.

$$T_{fp} = \left(1.477 \times NBP^{0.79686} \times \triangle H_{vap}^{0.16845} \times C_{num}^{-0.05948}\right) - 278.15$$

$$(2)$$

2.4 O-Ring Swelling *via* Hansen Solubility Parameters

O-ring swelling behavior of cycloalkanes were investigated by using the framework provided by Hansen (1967). The framework, called Hansen Solubility Parameters (HSP), relies on the ability to calculate a dispersion, polar, and hydrogen bonding term. These terms form the basis of a three coordinate system, often called Hansen space. Molecules can be plotted using this coordinate system, and the closer two molecules are on this space, the more alike they are. The framework provided by HSP allows for the determination of the likelihood of o-ring swelling. The more alike a cycloalkane is with a polymer, the more likely the cycloalkane can permeate through the polymer and cause o-ring swelling. Once the three HSP are known, the distance between two molecules (Ra) can be calculated as follows:

$$Ra^2 = 4\left(\delta_{d2} - \delta_{d1}\right)^2 + \left(\delta_{p2} - \delta_{p1}\right)^2 + \left(\delta_{h2} - \delta_{h1}\right)^2 \qquad (3)$$

Each polymer also has an interaction radius (Ro) ascribed to it. For a cycloalkane and a polymer, if Ra/Ro is less than 1, the two molecules a alike, and o-ring swelling behavior is predicted to occur. If Ra/Ro is greater than 1, then the two molecules are not alike, and o-ring swelling is not predicted to occur. One important aspect of cycloalkanes is that they are not very polar, and they do not hydrogen bond with other hydrocarbon cycloalkanes. This simplifies **Eq. 3**, where now, only the first term is important. In this work, the dispersion term is calculated through the following equation:

$$\sqrt{\frac{H_{vap}}{V_m}} \qquad (4)$$

where, H_{vap} is the standard enthalpy of vaporization, and V_m is the molar volume at 25°C.

2.5 Experimental Methodology

All chemicals and solvents were obtained from commercial sources and used as received unless otherwise specified. $NbOPO_4$ was heated to 100°C in a vacuum oven overnight prior to use. ^1H and ^{13}C NMR spectra were collected at room temperature on a Bruker AV400 MHz spectrometer, with chemical shifts referenced to the residual solvent signal. GC-MS analysis was carried out using an Agilent 7890 GC system equipped with an Agilent 5975 mass selective detector, a flame ionization detector (FID) and a Polyarc system. The Polyarc system is a catalytic microreactor that converts all organic compounds to methane after chromatographic separation and prior to detection.

Combustion calorimeter measurements were performed using an IKA C1 compact combustion calorimeter. Higher heating values were measured in triplicate using approximately 0.3 g sample and averaged. The lower heating values (reported as the specific energy) were calculated by subtracting the contribution due to hydrogen content from the higher heating value. Flash point was measured on an Ametek Miniflash FP flash point tester according to ASTM D6450 (ASTM D6450, 2021). In each run, around 1 ml of sample was injected into the sample cup and the heating rate was set to 5.5°C/min. Viscosity and density measurements were performed using an Anton Paar SVM 3001 according to ASTM D7042 (ASTM D7042, 2021) and ASTM D4052 (ASTM D4052, 2019). Freeze point (ASTM D5972) (ASTM D5972, 2016) and other cold flow properties such as cloud point (ASTM D5773) (ASTM D5773, 2021) and pour point (ASTM D5949) (ASTM D5949, 2016) were measured using Phase Technology PSA-70Xi-FP analyzer. Elemental analyses were performed by Atlantic Microlabs, Inc. (Norcross, GA, United States). Cyclohexane, cycloheptane, cyclooctane, cyclododecanone, cyclopentadecanone, (s)-(-)-limonene, and γ-terpinene were purchased from Sigma Aldrich. β-pinene and β-caryophyllene were purchased from Floraplex.

2.5.1 Synthesis of Cyclododecane

A 50 ml stainless-steel reactor was charged with cyclododecanone (2.00 g; 0.0109 mol), $Ni/SiO_2-Al_2O_3$ (20 wt%; 0.400 g), $NbOPO_4$ (50 wt%; 1.00 g), and hexane (12 ml). The reactor was sealed and pressurized with 300 psi H_2, flushing three times. The vessel was placed in a preheated aluminum block at 180°C and heated for 21 h with stirring. The reactor was cooled in a water bath until reaching room temperature and depressurized. An aliquot of the reaction mixture was filtered and analyzed by GC-MS, confirming complete consumption of cyclododecanone and formation of alkane products. The reaction mixture was filtered through a Celite plug into a vial containing ~1 g of $MgSO_4$ and the volatiles were removed under reduced pressure, yielding a white semi-solid (1.74 g; 0.0103 mol; 94% yield). ^1H NMR (400 MHz, $CDCl_3$): 1.35 ppm (singlet). ^{13}C NMR (100 MHz, $CDCl_3$): 23.84 ppm (singlet). GC-MS: m/z = 168.1 (retention time = 11.13 min).

2.5.2 Synthesis of Cyclopentadecane

A 50 ml stainless-steel reactor was charged with cyclopentadecanone (2.00 g; 0.009 mol), $Ni/SiO_2-Al_2O_3$ (20 wt %; 0.400 g), $NbOPO_4$ (50 wt%; 1.00 g), and hexane (12 ml). The reactor was sealed and pressurized with 300 psi H_2, flushing three times. The vessel was placed in a preheated aluminum block at 180°C and heated for 21 h with stirring. The reactor was cooled in a water bath until reaching room temperature and depressurized. An aliquot of the reaction mixture was filtered and analyzed by GC-MS, confirming complete consumption of cyclopentadecanone and formation of alkane products. The reaction mixture was filtered through a Celite plug into a vial containing ~1 g of $MgSO_4$ and the volatiles were removed under reduced pressure, yielding a white semi-solid (1.60 g; 0.0085 mol; 96% yield). ^1H NMR (400 MHz, $CDCl_3$): 1.33 ppm (singlet). ^{13}C NMR (100 MHz, $CDCl_3$): 27.03 ppm (singlet). GC-MS: m/z = 210.2 (retention time = 12.34 min).

2.5.3 Hydrogenation of Terpenes

The hydrogenation of terpenes was carried out in a 50 ml stainless-steel reactor. Typically, 5 g of terpene was placed in the reactor, which was purged with hydrogen gas three times. For β-pinene and β-caryophyllene, 10% Pd/C (10 wt%) was added to the reactant, while for (s)-(-)-limonene and γ-terpinene 5% Pt/C (10 wt%) was added to the reactant. The reactor was charged with 200 psi H_2, after H_2 was completely consumed, the reactor was re-charged with H_2 based on the calculated H_2 consumption required for complete hydrogenation of 5 g of a terpene. An aliquot of the reaction mixture was filtered and analyzed by GC-MS and NMR, confirming complete hydrogenation and formation of saturated products. The reaction mixture was filtered through a Celite plug into a vial, and the resulting products were used without further purification.

3 RESULTS AND DISCUSSION

The computational methods used to make predictions have been previously shown to yield accurate results. With respect to specific energy and energy density, the literature shows that the enthalpies calculated with the CBS-QB3 method have a RMSD (Root Mean Square Deviation) of 1.49 kcal mol^{-1} (Pokon et al., 2001). To understand how the accuracies of enthalpies translates to accurate specific energy and energy density the specific energy and energy density were calculated for a set of hydrocarbons. The absolute average deviation (AAD) was found by comparing the predicted values to measured values from the literature (Heyne, 2018). The AAD for specific energy and energy density were found to be 0.35 MJ/kg, and 0.51 MJ/L, respectively. This is in accord with the reproducibility quoted in the ASTM standard for specific energy, ASTM-D240, of 0.4 MJ/kg (ASTM D240, 2019). Results of this analysis are shown in **Supplementary Table S1**. Although there is a systematic underprediction in the specific energy using CBS-QB3 is accurate such that predictions of the specific energy fall within the error bars of experimentally determined values.

Part of the process of predicting the energy density involves predicting the physical density of the target molecule. The density of each target molecule is calculated using the SAFT-γ-Mie EoS.
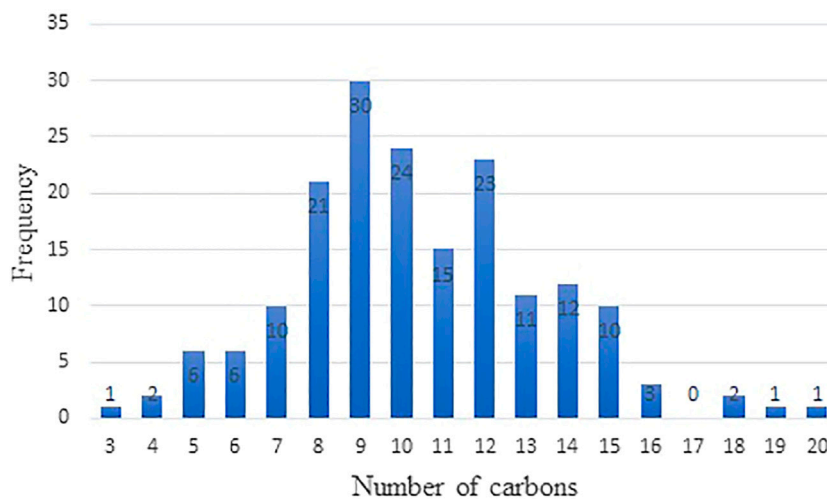
FIGURE 1 | Distribution of cycloalkanes in the database as a function of the number of carbons in the cycloalkane.

SAFT-γ-Mie consistently yields accurate densities throughout the full liquid range of simple and complex mixtures, and variants of it have been used for decades (Chapman et al., 1989; Gross and Sadowski, 2002; Abala et al., 2021). Additionally, in 2017 Perez et al. published a comparison study between different EoS approaches to evaluate predictions of VLE (Vapour-Liquid Equlibria), and density for pure and binary mixtures commonly found in carbon-capture sequestration work (Chapman et al., 1989). This study relied on 22,904, 26,479, and 31,928 measurements of VLE, binary mixture density, and single-phase density, respectively. Perez et al. (2017) concluded that SAFT EoSs methods for predicting density had accuracies better than 3.0% AAD% (Percent Absolute Average Deviation) for all chemical systems studied, and an average AAD% of 1.16. All data taken together, the SAFT EoS was superior to other EoS methods studied.
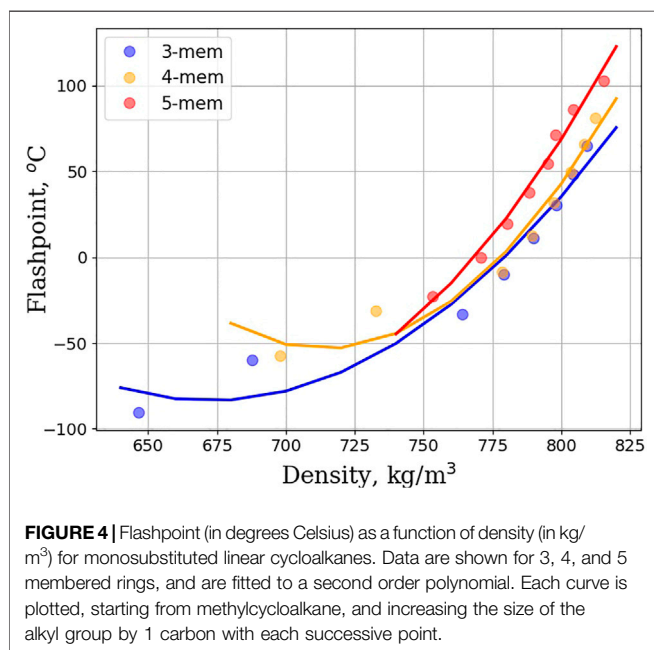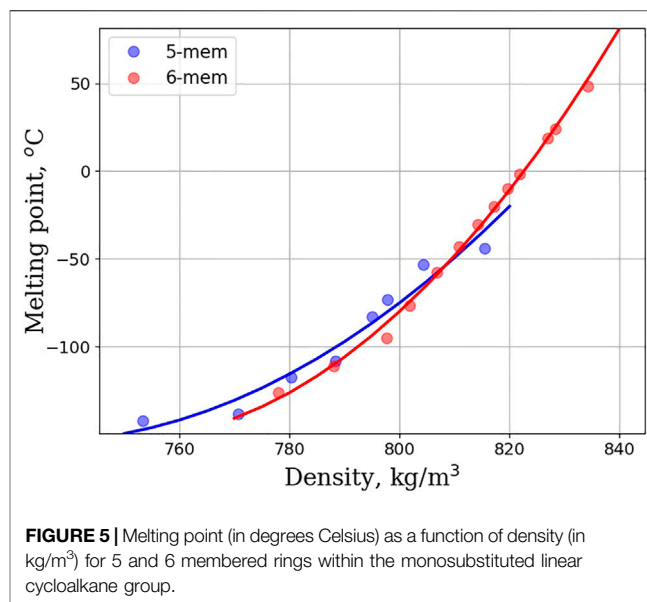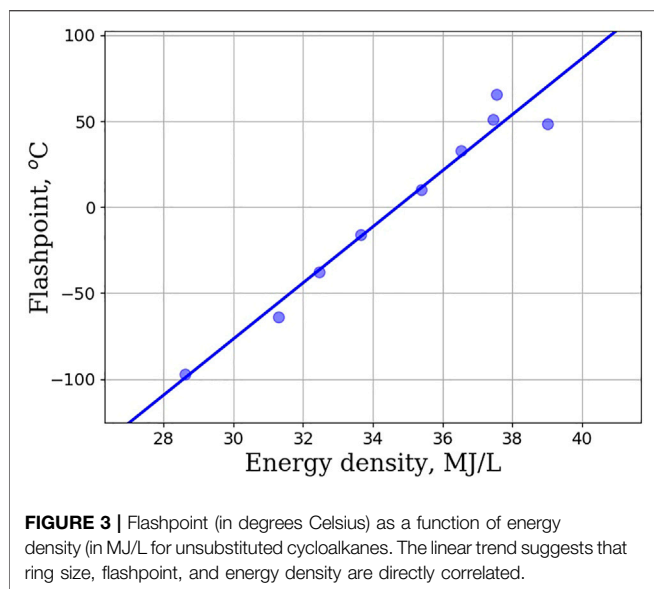
178 cycloalkane structures were examined in this study. **Figure 1** plots the number of cycloalkane structures in the database with the number of carbons in the structure. The maximum of the distribution occurs at a carbon number of 9, for which we have 30 structures. A second peak occurs with structures containing 12 carbon atoms. This distribution is lighter than the distribution of petroleum based jet fuels where molecular structures containing 9 to 16 carbon atoms is typical. The distribution found in **Figure 1** broadly represents components found in jet fuel (Corporan et al., 2011). Melting points given here were taken from published databases and the open literature (Acree and Chickos, 2011; Bradley and Andrew, 2014; Rosenkoetter et al., 2019; Muldoon and Harvey, 2020). Unfortunately, not every cycloalkane in the database has a melting point value. There are no accurate prediction tools available for melting point, and melting points were only taken from databases and the open literature. In the next few sub-sections basic SPR are shown which, together, start to reveal the relationship between structure and function that lead to good jet fuel performance.
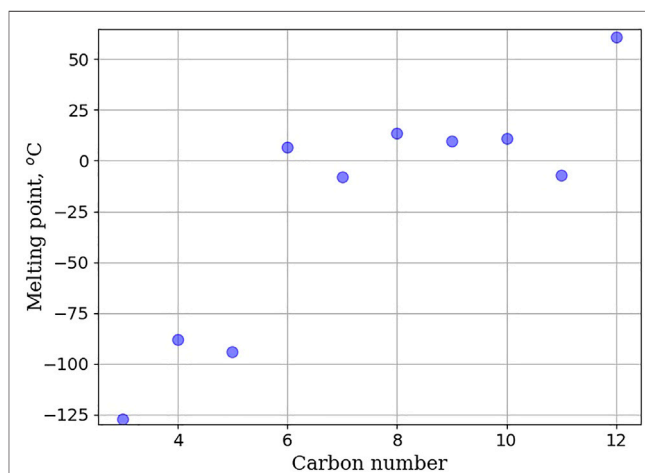
FIGURE 2 | Plot of melting point as a function of the number of carbons in the ring of the cycloalkane. Melting point of unsubstituted cycloalkanes do not increase linearly, but rather reach a plateau between cyclohexane and cyclodecane before increasing to 61°C.

3.1 Unsubstituted Cycloalkanes

Figure 2 shows the melting point of unsubstituted rings as a function of the number of carbon atoms in the ring. Rings larger than 5 carbon atoms fail to meet the melting point specification for Jet-A. Melting point does not increase monotonically but rather reaches a plateau between 6 and 10 carbon atoms, before decreasing slightly, and then increasing to a melting point of 61°C, for cyclododecane. Drotloff and Moller used DSC (Differential Scanning Calorimetry) to investigate the phase transition of large cycloalkane rings (Drotloff and Moller, 1987). They observed that melting point behavior is correlated to the amount of disorder in the liquid phase and that cycloalkanes with lower ring strain can adopt multiple, different conformations. The degree to which these conformations can be accessed influences the melting point.

FIGURE 3 | Flashpoint (in degrees Celsius) as a function of energy density (in MJ/L for unsubstituted cycloalkanes. The linear trend suggests that ring size, flashpoint, and energy density are directly correlated.

FIGURE 5 | Melting point (in degrees Celsius) as a function of density (in kg/m³) for 5 and 6 membered rings within the monosubstituted linear cycloalkane group.

FIGURE 4 | Flashpoint (in degrees Celsius) as a function of density (in kg/m³) for monosubstituted linear cycloalkanes. Data are shown for 3, 4, and 5 membered rings, and are fitted to a second order polynomial. Each curve is plotted, starting from methylcycloalkane, and increasing the size of the alkyl group by 1 carbon with each successive point.
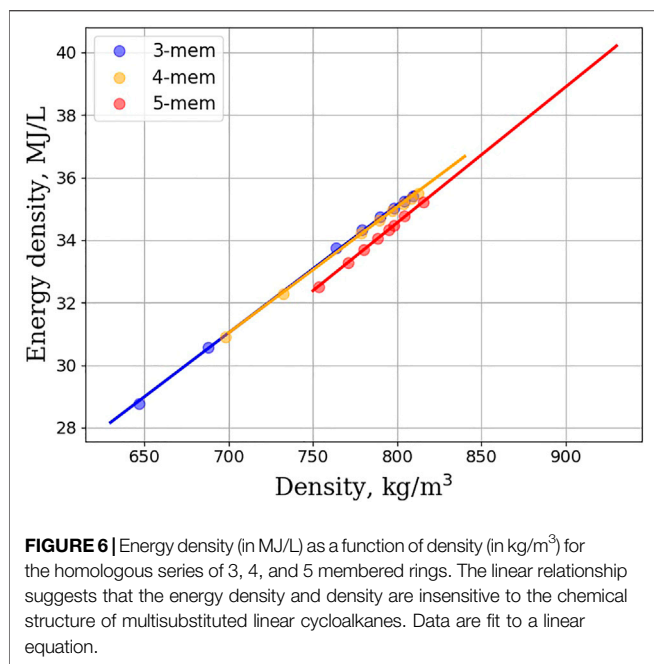
Figure 3 shows the variation in flashpoint as a function of energy density. This relationship is mostly linear, with deviations occurring with larger ring sizes. The low energy density for small rings (cyclopropane and cyclobutane) is a byproduct of their much smaller densities. Conversely, their high specific energies are a results of their higher ring strain, which when broken releases more energy (Sirjean et al., 2006). The inference drawn from **Figure 3** is that as ring size increases benefits to flashpoint and energy density are obtained. Unsubstituted cycloalkanes can be used in the design of SAFs so long as they are included as blends or contain other structural features that can decrease their melting point. **Supplementary Tables S2–S5**

shows experimental values for blending unsubstituted rings with Jet-A (POSF-10325) at 10 wt%. All blends meet the Jet-A specification for freeze point, viscosity, and specific energy. This is contrary to the neat cycloalkane physical properties where all of the cycloalkanes fail to meet the jet-A specification for melting point. In addition, pure solutions of cyclohexane, cycloheptane, and cyclooctane fail to meet jet-A specification for flashpoint. The data show that as modest (10 wt % blends), unsubstituted cycloalkanes can lead to acceptable jet-A fuels. Unfortunately, data for higher blends are not promising. **Supplementary Tables S6–S9** show experimental measurements for unsubstituted cycloalkanes blended into Jet-A (POSF-10325) at 30 wt%. 30 wt% blends fail to meet many of the Jet-A specifications. The cyclododecane blend fails to meet the freeze point specification, the cyclohexane and cycloheptane blend fail to meet the flashpoint requirement, and the cyclododecane and the cyclopentadecane blend fail to meet the viscosity requirement for Jet-A. All unsubstituted cycloalkanes studied fail to meet at least one of the requirements for Jet-A, and at 30 wt% blends, unsubstituted rings cannot be used.

3.2 Monosubstituted Linear Cycloalkane

An alternative route to meet Jet-A specification is to add alkyl substituents to unsubstituted cycloalkane rings. **Figure 4** shows the flashpoint vs. density plot for monosubstituted linear cycloalkanes. The homologous series of 3, 4, and 5 membered rings is depicted, and a clearly discernable trend is that as density increases so too does the flashpoint. Strikingly, the curves for 3, 4, and 5 membered rings are nearly overlapping, suggesting that ring size plays little to no role in this trend. **Figure 5** shows the density vs. melting point for the homologous series of 5 and 6 membered monosubstituted linear cycloalkanes. The literature shows that the orientational dependence, upon freezing, plays a large role in understanding the melting properties of monosubstituted linear cycloalkanes. Hasha and Huang

FIGURE 6 | Energy density (in MJ/L) as a function of density (in kg/m^3) for the homologous series of 3, 4, and 5 membered rings. The linear relationship suggests that the energy density and density are insensitive to the chemical structure of multisubstituted linear cycloalkanes. Data are fit to a linear equation.

observed a coupling between the rotational and translational motion of methylcyclohexane using NMR (Hasha and Huang, 1979). They postulated that this coupling plays a large role in the melting properties of methylcyclohexane. The crystal structure of methylcyclopentane was investigated and found to be oriented in an envelope conformation, with the methyl group adopting a pseudo-equatorial position (Bream et al., 2006). Upon freezing, the methylcyclopentanes adopt a zig-zag pattern with each other, with some methyl groups pointed diagonally upwards, and some pointed diagonally downwards. Finally, Milhet et al. used DSC to observe the melting behavior of n-alkyl cyclohexanes. Their observations revealed that melting temperature increases as chain length increases, but that odd carbon length chains behaved differently from even carbon length chains (Milhet et al., 2007). Adding an extra CH2 to an alkyl chain with an odd number of carbons increased the melting temperature more than if a CH2 was added to an alkyl chain length with an even number of carbons. This suggests that indeed orientational dependence does play a role, but that as alkyl chain length increases the number of orientations that can be adopted in a crystalline structure decreases, and solidification becomes easier. The plot in **Figure 5** captures this orientational dependence by plotting the density and shows that melting point increases as the linear alkane length increases. The linear relationship between density and energy density is shown in **Figure 6**. For all homologous series studied, the energy density is a linear function of the density and if large energy densities are desired, large densities are needed. The conclusions drawn from **Figures 4–6** are that density is an overriding factor in determining what role monosubstituted linear cycloalkanes can play in the generation of SAFs. Higher densities lead to higher energy densities, but at the expense of higher melting points, and trade-offs are required to ensure that existing fuel requirements

are met. If a mixture of simple linear cycloalkanes were generated with densities at the top range of the jet-A specification (840 kg/m^3), such a mixture would likely fail to meet the jet-A specification for melting point. **Figure 6** indicates that it would have a melting point estimate of >50°C. In order to meet the melting point specification, it would need to have a density < ~810 kg/m^3.
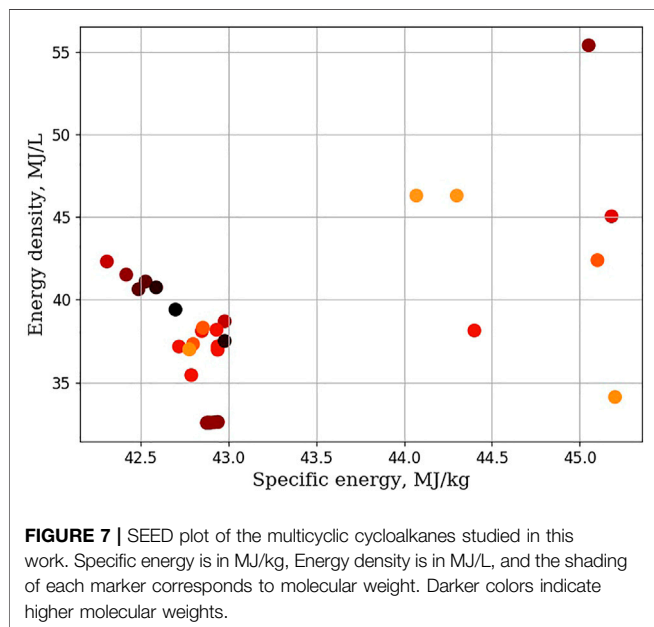
3.3 Polysubstituted Linear Cycloalkane

Due to the structural complexity available in this group, there are no easily identifiable trends within the data however, all structures exceed the minimum Jet-A specification for specific energy of 42.8 MJ/kg. A few cycloalkanes in this group are notable in that they have specific energy in excess of 0.5% above the median Jet-A while achieving comparable energy density. These structures, and their properties are shown below in **Table 2**. A pattern that emerges from this data is that multiply substituted molecules with rings greater than 6 carbons are suitable cycloalkanes for the development of SAFs. These are suitable molecules, because they feature large densities and flashpoints while maintaining very low melting points. In addition, although viscosity is not covered in this work, there is evidence in the literature that they can have good viscosities (Rosenkoetter et al., 2019). A mixture of 1,4 and 1,5 dimethylcyclooctane was prepared using a [4 + 4] cycloaddition of isoprene catalyzed by an Iron catalyst (Rosenkoetter et al., 2019). Measured physical properties of this mixture show that its freezing point is <−78°C, and its viscosity at −20°C is 4.17 mm^2/s (Rosenkoetter et al., 2019). These values are well below the maximum value for Jet-A, as indicated in **Table 1**. The structural reasons for why polysubstituted ring expanded cycloalkanes have good cold flow properties is not known, but, as discussed previously, it may be related to greater flexibility conferred by the addition of multiple alkyl chains to the ring. Running quantum mechanics calculations on 1,4-dimethylcyclooctane, the lowest energy configuration is the crown configuration. This is different from the boat-chair conformation adopted by cyclooctane. Another pattern that emerges from the data is that cyclic structures which have di-methylated carbon atoms can have very good physical properties.

3.4 Monosubstituted and Polysubstituted Branched Cycloalkanes

The main biological route to branched cycloalkanes is through the MEP pathway. Using computational modeling the production of limonene in cyanobacteria was increased 100 fold (Wang et al., 2016). The computational modeling identified a bottleneck to the production of limonene, which once removed, allowed for increased limonene production. Through genetic engineering of *R. turuloides* researchers were able to achieve titers of α-bisabolene and 1,8-cineole of 2.6 and 1.4 g/L, a several fold increase over previously reported efforts (Kirby et al., 2021). Chemical routes reported in the literature are sparse and rely on reduction of a starting oxygenate. Starting from diacetone alcohol, a dehydration/diels alder process was developed, which when hydrogenated furnished a mixture of

Chemical name	SE, MJ/kg	ED, MJ/L	MP, °C	Density, kg/m^3	Flashpoint, °C
1,1-diethylcyclohexane	43.60	35.81	−54.4	828.60	49.20
1,2,3,4-tetramethylcyclohexane	43.26	35.4	−75	825.80	40.50
1,4-dimethylcyclooctane	43.82	36.22	−78	827.00	49.50
1,1,4-trimethylcycloheptane	43.56	34.83	***	807.60	42.50
1,1,5-trimethyl-2-pentylcyclohexane	43.46	35.00	<−75	812.60	***

FIGURE 7 | SEED plot of the multicyclic cycloalkanes studied in this work. Specific energy is in MJ/kg, Energy density is in MJ/L, and the shading of each marker corresponds to molecular weight. Darker colors indicate higher molecular weights.

cyclopentanes. Branched cyclopentanes were a major fraction of the products formed, and the overall mixture has a freezing point of −56.6°C (Chen et al., 2016a). Starting from a lignocellulosic oxygenated by product, hydrodeoxygenation afforded a 12 C branched cycloalkane (Li et al., 2020). One important feature of branched cycloalkanes is their low melting points. In the database, constructed for this paper, isopropyl and isobutyl substitutions lead to melting points of at least 50°C below the jet-A specification. Tert-butyl linkages also have good melting points, but tert-butylcyclohexane's melting point of −41.2°C hovers just below the jet-A specification. No melting point data outside of 5 and 6 membered rings are available hence, a correlation between ring size and branching substituent is not possible. Of the branched cycloalkanes examined, specific energies increased by an average of 1.04%, and energy densities fell by an average of 1.73% over median jet-A values. The molecules with the highest specific energies were those with an isopropyl group. Most molecules with a tert-butyl group showed the largest decreases in energy density. Reasons for this include lower specific energies, but also lower physical densities.

Polysubstituted branched cycloalkanes do not show any benefit over monosubstituted branched cycloalkanes. Specific energies and energy densities calculated are commensurate with those calculated for monosubstituted branched

cycloalkanes. Additionally, not a lot is known about the melting points of polysubstituted branched cycloalkanes. Further, because they have multiple substitution sites, they are likely to have higher YSI yields. Given the difficulty of producing polysubstituted branched cycloalkanes, it is unlikely that there will be benefits to including them in SAFs.

3.5 Multicyclic-Cycloalkanes

The SEED plot for molecules in the MC group are shown in **Figure 7**. Most multicyclic molecules are located within a band bounded between 42 and 43 MJ/kg, and 33 and 43 MJ/L. The remaining seven molecules are cis-carane, and a group of molecules that belong to a class of molecules called ladderanes. Further, there is no correlation between molecular weight and where a molecule falls in the SEED plot. This finding indicates that the type of carbon-carbon bond is important, and that low molecular weight, ring strained molecules can lead to elevated energy densities and specific energies. Focusing on decalins, in 2009, researchers using an ignition quality tester, IQT, determined that the cetane number of cis-decalin was significantly higher than trans-decalin (Hasha and Huang, 1979). Although cis-decalin does not have great physical properties for jet fuel, the authors suggested those physical properties may be improved by adding a single isoparaffin group to the cis-decalin core (Heyne et al., 2009). Also, in 2019 researchers upgraded cyclopentanone to a series of alkyl-decalins. The measured freezing point of the isomerization mixture was reported to be −23.45°C. In this work, several derivatives of cis-decalin were evaluated as possible candidates for inclusion into SAFs. **Table 3** lists these derivatives along with their physical properties. Cis-decalin has a measured energy density of 38.7 MJ/L. This is 10.8% higher than the median Jet-A value. However, its specific energy of 42.98 MJ/kg is 0.51% lower than the median Jet-A value. As a jet fuel component, its melting point of −38.8°C is slightly above the −40°C upper limit of the jet-A fuel specification, and has a low temperature viscosity, at −20°C, of 11.3 mm^2/s (see **Table 1**). In this work, a series of dimethyl cis-decalins have been evaluated. The physical properties of cis-decalin, and its derivatives, are tabulated in **Table 3**. Dimethyl cis-decalins have lower densities and thus lower energy density than cis-decalin. A 2016 paper outlined a conversion strategy, starting from cyclopentanol, which generated a mixture of C10 decalin and C15 polycycloalkanes. Measured physical properties of this mixture show that it has a melting point that is less than −110°C, and a density, measured at 20°C, of 876 kg/m^3 (Chen et al., 2016b). The clear suggestion here is that decalin mixtures can yield promising

TABLE 3 | Physical properties of cis-decalin and some dimethyl-decalins analyzed in this work.

Chemical name	Specific energy, MJ/kg	Energy density, MJ/L	Melting pt. °C	Density at 15°C kg/m³
cis-decalin	42.98	38.70	-38.80	901.02
1,10-dimethyl-cis-decalin	42.90	32.56	***	***
1,2-dimethyl-cis-decalin	42.94	32.60	***	***
1,3-dimethyl-cis-decalin	42.88	32.55	***	***
1,4-dimethyl-cis-decalin	42.89	32.56	***	***
1,5-dimethyl-cis-decalin	42.88	32.55	***	***
1,6-dimethyl-cis-decalin	42.92	32.58	***	***
1,7-dimethyl-cis-decalin	42.88	32.55	***	***
1,8-dimethyl-cis-decalin	42.94	32.60	***	***

TABLE 4 | Physical properties of octahydropentalene and its derivatives analyzed in this work.

Chemical name	Specific energy, MJ/kg	Energy density, MJ/L	Density at 15°C kg/m³
Octahydropentalene	42.78	37.00	873.50
methyl-octahydropentalene	42.86	38.31	902.67
ethyl-octahydropentalene	42.93	38.18	897.67
propyl-octahydropentalene	42.98	38.06	893.56
sec-butyl-octahydropentalene	42.95	37.95	891.47

physical properties. However, SAF generating process are unlikely to derive large benefits from the inclusion of dimethyl cis-decalins. Adding larger alkyl substituents, like an n-butyl substituent to cis-decalin recovers most of the density lost from alkylation of cis-decalin, but likely have melting points that are too high to be useful as SAF components. Of course, cis-decalin is not the only fused bicyclic compound available. Other bicyclic compounds, such as octahydropentalene (two fused cyclopentanes), and mixed cyclic fused molecules are also available. **Table 4** shows the physical properties for octahydropentalene and its derivatives. Octahydropentalenes show only modestly higher specific energy values but show elevated energy density. Additionally, they show densities that are too high to meet Jet-A requirements. Octahydropentalene's flashpoint is 20.7°C, 17.3°C below the Jet-A specification. It is likely that octahydropentalenes will require blending to meet the requirements for Jet-A fuel. Octahydropentalene can be chemically synthesized through a number of routes (Gunbas et al., 2005). Further, iodination and bromination can serve as sites for further derivatization by alkyl substitution (Gunbas et al., 2005). Other derivatizations are also possible (Kendhale et al., 2008). A biological pathways to octahydropentalene derivatives is available, starting from glycerol (Li et al., 2014). Some work has been reported on other fused rings containing 5 and 6 membered rings. Starting from aromatic aldehydes and methyl isobutyl ketone a pathway to the formation of octahydroindanes was reported (Muldoon and Harvey, 2020). The route yields a mixture that has a freezing point that hovers around the −40°C upper limit and features a density of 885 kg/m³. The formation of a binary mixture of perhydrofluorene and dicyclohexamethane from aromatic building blocks, yielded a melting point of −40°C, and a density of 930 kg/m³ (Muldoon and Harvey, 2020). A class of

molecules called ladderanes consist of fused cyclobutanes. They can be prepared chemically in a variety of ways, and are natural products produced by planctomycetes. Anammox planctomycetes, which is the species responsible for producing ladderanes, plays an important part in the remediation of nitrogen-rich wastewater. **Table 5** shows the ladderane structures examined in this work, along with the measured and predicted physical properties. Ladderanes, even the simples bicyclic ladderane, possess remarkably high specific energy and energy density. An analysis from NIST reveals that the bicyclic ladderane possesses a viscosity of 0.77 mm²/s at −13.15°C (Kazakov et al., 2002). It is likely therefore, that it meets the maximum viscosity of 8 mm²/s at −20°C. Further, the density of the bicyclic ladderane at 15°C is 828.2 kg/m³, below the maximum of 840 kg/m³. When the bicyclic ladderane is alkylated, our work shows that the energy density increases while the specific energy remains elevated. This suggests that alkylation of ladderanes can serve as routes to improve physical properties.

Strained, multicyclic cycloalkanes are also possible. In the literature, these are often hydrogenated terpenes, and in this work, those which were studies, along with their physical properties, are tabulated in **Supplementary Table S13**. Cis-carane, pinane, and sabinane all have the same chemical formula (C10H18). Cis-Carane has higher specific energy and energy density values, and has a viscosity, measured at −40°C, of 6.83 mm²/s, and a density, measured at 15°C, of 842 kg/m³. Pinane has somewhat lower specific energy and energy density, compared to cis-carane, but still higher than the median value of Jet-A fuels. At −40°C, the viscosity of pinane is 11.23 mm²/s, and has a freeze point of −53°C. Its flashpoint is 39.7°C.

Blends of hydrogenated terpenes can often be beneficial. Experimental measurements using 10 and 30 wt % of pinane,

TABLE 5 | Physical properties of ladderanes and their derivatives analyzed in this work.

Chemical name	Specific energy, MJ/kg	Energy density, MJ/L
Ladderane Sims et al. (2014)	44.60	42.30
Ladderane ASTM D756 (2015), syn	44.30	46.30
ladderane ASTM D7566 (2015), anti	44.07	46.30
dimethyl-ladderane Sims et al. (2014)	45.20	34.12
isopropyl-ladderane Sims et al. (2014)	45.10	42.39
diethyl-ladderane Sims et al. (2014)	45.18	45.05
dipropyl-ladderane Sims et al. (2014)	45.05	55.40

TABLE 6 | Hansen Solubility Parameters, average Ra/Ro, and standard deviations for the polymers and cycloalkane data set analyzed in this work. Standard deviations are very low, indicating that most cycloalkanes either exhibit o-ring swelling, or do not. HSP data taken from Accu Dyne Test.

Polymer material	δD	δP	δH	Average Ra/Ro	Std. dev.
Fluorocarbon	14.6	10	1.6	1.25	0.08
Silicon	13.8	5	1.2	0.53	0.09
Poly(acrylonitrile)	21.7	14.1	9.1	1.81	0.08
Poly(butadiene)	17.5	2.3	3.4	0.73	0.10
Acrylonitrile butadiene styrene (ABS)	17	5.7	6.8	0.97	0.03
Epoxies	19.2	10.9	9.6	1.40	0.05
Fluorinated ethylene polypropylene	19	4	3	1.78	0.28

carryophyllane, limonene, and p-menthane were carried out. Blends were generated using the POSF 10325 Jet-A fuel. **Supplementary Tables S10–S13** shows the neat physical properties of these hydrogenated terpenes, followed by their blended physical properties. The viscosity of pinane at −40°C is 12.256 mm²/s, which is at the border of pass/fail. At 10 wt% blends with Jet-A, the viscosity is measured to be 8.94 mm²/s, within the Jet-A specification. Carryophyllane fails to meet viscosity requirements for Jet-A. As a 10 wt% blend, it still fails to meet viscosity specification. Smaller blends are possible, but will dilute the elevated energy density and specific energy neat values of carryophyllane. Limonane and terpinane have neat properties that meet Jet-A specifications. As blends, low temperature viscosities increase, specific energies decrease, and flashpoints increase. In this scenario, a trade-off needs to be made between decreasing specific energy and increasing flashpoints.

3.6 O-Ring Swelling

O-ring swelling behavior was inspected by using the framework provided by Hansen Solubility Parameters (HSP). This framework allows for the identification of molecules with similar interactional forces. It is described in further detail in the methodology section. A number of polymer materials were analyzed, and the results of the analysis are shown in **Table 6**. HSPs were obtained from (Accu Dyne Test, 2021) Polymers which have a Ra/Ro that is less than 1 indicate that o-rings made out of that polymer will exhibit o-ring swelling behavior when exposed to cycloalkanes. Polymer materials with low polarity and hydrogen bonding terms, but a high dispersion term show the best promise for o-ring swelling behavior. All cycloalkanes studied indicate they will produce o-ring swelling in o-rings made from polybutadiene. Di methyl and tri methyl
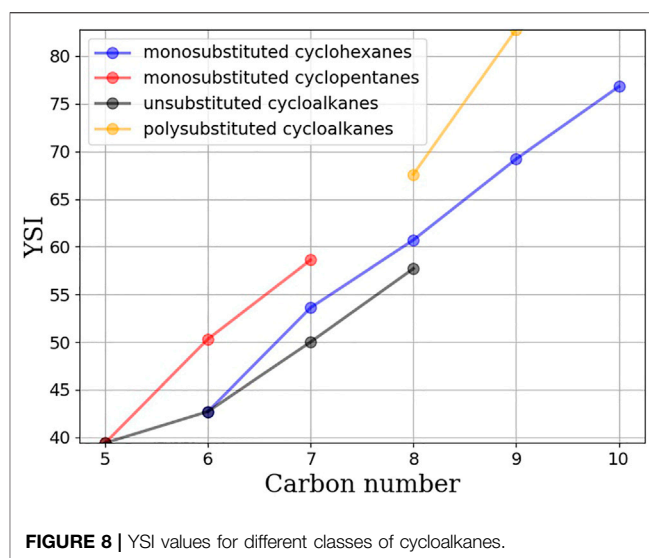
cyclohexanes and cyclopentanes show Ra/Ro values that were closest to 1, indicating that they may produce minimal amounts of o-ring swelling. Ra/Ro values were all significantly above 1 for o-rings made with polyacrylonitrile polymers, indicating that cycloalkanes are less likely to induce o-ring swelling in polyacrylonitrile than in polybutadiene. The best performing cycloalkanes were fused cycloalkanes. Octacyclopentalene (two five membered rings fused together), and decahydro-1H-cyclopenta[a]pentalene (three five membered rings fused together) were best performers. Research has indicated that disruption of the interaction of nitrile groups is important to inducing o-ring swelling. Although no definitive conclusions can be drawn, it appears that many of the cycloalkanes studied do not possess the ability to disrupt these interactions in acrylonitrile. O-ring swelling in acrylonitrile-butadiene-styrene polymers were also examined, by analyzing the results of HSP. Results indicate that cycloalkanes may produce some o-ring swelling in o-rings made from acrylonitrile-butadiene-styrene material. Ra/Ro values hover around 1. It is unclear which cycloalkanes may provide o-ring swelling. The standard deviation is small (0.03), and because of uncertainty it is difficult to ascertain which cycloalkanes may be considered best performers. Overall, what can be said of this analysis is that fused cycloalkanes tend to provide the best opportunities for o-ring swelling. This seems to be true regardless of the o-ring material. This does not mean that o-ring swelling is guaranteed, merely that fused cycloalkanes provide the best opportunity to induce sufficient o-ring swelling. Future experimental work may shed more light, but computational simulations may also aid in understanding the criteria necessary for cycloalkanes to induce o-ring swelling in different materials. Some of the molecules studied in this work have physical properties that are at least commensurate with those of Jet-A. As blends, these molecules offer the best

opportunities for providing adequate o-ring swelling while maintaining the physical properties of the blended fuel.

3.7 Sooting Propensity

Aromatics are well known to contribute substantially to soot production during combustion compared to most non-aromatic compounds found in conventional jet fuel (Aromatics perform an important seal-swelling function in jet fuel, and cyclic alkanes have been proposed as an alternative for aromatics to perform the seal-swelling function.). A number of indices have been developed to quantify the relative tendency of hydrocarbons to produce soot. One of the earliest indices, Smoke Point (SP), has been used since the 1930's (Woodrow, 1933), and the measurement involves observing a flame from a standard lamp and measuring the fuel consumption rate (Schalla and McDonald, 1953) or flame height at which visible smoking occurred with lower SPs intended to indicate a greater tendency to produce soot. Systematic measurements of different molecular classes revealed qualitative structure property relationships for SP (Hunt, 1953; Calcote and Manos, 1983) with the general trend in sooting tendency following the pattern: n-paraffins < iso-paraffins < cycloalkanes < alkenes < alkynes < benzenes < naphthalenes. The Threshold Sooting Index (TSI) index was subsequently developed to provide an approximate adjustment for variations in SP related to the quantity of air consumed during combustion, with TSI defined as aMW/SP+b where MW is the molecular weight of the fuel and a and b are constants assigned through measurements of standard compounds to put all TSI measurements on a common scale. Using TSI values the additional trend if increasing soot tendency with increasing carbon number could be seen within different classes of hydrocarbons. In order to improve the reproducibility and precision of sooting tendencies compared to TSI values researchers have subsequently developed other indices that do not rely on SP measurements including Yield Sooting Index (YSI) (McEnally and Pfefferle, 2007; YSI database v2, 2021), Micropyrolysis Index (MPI) (Crossley et al., 2008), and Fuel Equivalent Sooting Index (FESI) (Lemaire et al., 2015). Quantitative structure property relationships based on group contribution methods have been developed for YSI (Crossley et al., 2008; John et al., 2017; Lemaire et al., 2021) for predicting sooting tendencies of uncharacterized hydrocarbons on the basis of their chemical structure.

As a specific example we can look at YSI values, which are derived from the maximum volume-fraction of soot measured by laser induced incandescence along the centerline of a methane co-flow diffusion flames doped with small quantity a specific hydrocarbon. YSI values on the current unified scale (Das et al., 2018) are scaled to give a value of 30 for n-hexane and 100 for benzene. The current YSI database includes 16 cycloalkanes with species in four ring sizes: cyclopentane, cyclohexane, cycloheptane, and cyclooctane. For cycloalkanes with the same molecular weight, higher YSI values are measured for cycloalkanes with multiple substitutions compared to cycloalkanes with longer alkyl side chains. The highest YSI value for a cycloalkane in the database is 82.8 for 1,2,4-trimethylcyclohexane, and the

FIGURE 8 | YSI values for different classes of cycloalkanes.

lowest two are cyclohexane and cyclopentane at 42.7 and 39.4, respectively. By comparison, naphthalene has a value of 466.1. The trends in measured YSI values (YSI database v2, 2021) for different structural classes of cycloalkanes is shown in **Figure 8**.

In an effort to understand the potential of including cycloalkanes into SAFs, a database of cycloalkanes, and their physical properties was developed. This database contains 178 cycloalkane structures, and includes information on specific energy, energy density, liquid density, flashpoint, and HSP. From this database, SPRs were developed based on cycloalkane structural features. These structural features include ring size, monosubstituted linear substitutions, polysubstituted linear substitutions, monosubstituted branched substitutions, polysubstituted branched cycloalkanes, and multicyclic cycloalkanes. The SPR developed indicate that unsubstituted cycloalkanes are of limited usefulness for the production of SAFs, because of their high melting points. Experiments, blending unsubstituted cycloalkanes into Jet-A (POSF-10325), show that 10 wt% blends meet the specifications outlined by ASTM D1655, but 30 wt% blends do not. Linear alkyl substitutions can greatly decrease melting points, while maintaining suitably high specific energies and energy densities. In particular, polysubstituted linear, ring expanded cycloalkanes offer large benefits, in terms of exceptional melting points, and large specific energies and energy densities. However, due to their larger YSI values, careful consideration must be taken to avoid sooting issues. Branched substitutions can be beneficial to lowering melting point however, their specific energies and energy densities are only commensurate with median Jet-A values. Given the difficulty of generating (biologically or chemically) branched cycloalkenes, their inclusion into SAFs may be challenging. HSP show that fused cycloalkanes are consistently amongst the most likely cycloalkanes to provide o-ring swelling. For that reason, they should also be considered as possible jet-fuel cycloalkane candidates. Experimental measurements show that some fused cycloalkanes can meet jet-A standards, as specified by ASTM D-1655, especially as 10 and 30 wt% blends. However, not all fused cycloalkanes are good fuel component candidates.

Carryophyllane failed to meet Jet-A specifications, even at a modest 10 wt% blend into Jet-A (POSF-10325).

DATA AVAILABILITY STATEMENT

The raw data supporting the conclusion of this article will be made available by the authors, without undue reservation.

AUTHOR CONTRIBUTIONS

AL and RPB wrote manuscript. AL, RPB, SPD, and NH conducted research. CMM, ADS, and AG supervised research.

REFERENCES

Abala, I., Lifi, M., Alaoui, F. E. M., Munoz-Rujas, N., Aguilar, F., and Montero, E. A. (2021). Density, Speed of Sound, Isentropi Compressibility, and Refractive index of Ternary Mixtures of Oxygenated Additives and Hydrocarbons (Dibutyl Ether + 1-Butanol + Toluene or Cyclohexane) in Fuels and Biofuels: Experimental Data and PC-SAFT Equation-Of-State Modeling. *J. Chem. Eng. Data* 66, 1406–1424. doi:10.1021/acs.jced.0c01025

Accu Dyne Test (2021). Surface Free Energy Components by Polar/Dispersion and Acid-Base Analyses; and Hansen Solubility Parameters for Various Polymers. Available from: https://www.accudynetest.com/polytable_02.html (cited July 11, 2021).

Acree, W. E., and Chickos, J. S., (2011). Phase Transition Enthalpy Measurements of Organic and Organometallic Compounds.

ASTM D1655 (2019). *Standard Specification for Aviation Turbine Fuels*. West Conshohocken, PA: ASTM International. www.astm.org.

ASTM D240 (2019). *Standard Test Method for Heat of Combustion of Liquid Hydrocarbon Fuels by Bomb Calorimeter*. West Conshohocken, PA: ASTM International. www.astm.org.

ASTM D4052 (2019). *Standard Test Method for Density, Relative Density, and API Gravity of Liquids by Digital Density Meter*. West Conshohocken, PA: ASTM International. www.astm.org.

ASTM D5773 (2021). *Standard Test Method for Cloud Point of Petroleum Products and Liquid Fuels (Constant Cooling Rate Method)*. West Conshohocken, PA: ASTM International. www.astm.org.

ASTM D5949 (2016). *Standard Test Method for Pour Point of Petroleum Products (Automatic Pressure Pulsing Method)*. West Conshohocken, PA: ASTM International. www.astm.org.

ASTM D5972 (2016). *Standard Test Method for Freezing Point of Aviation Fuels (Automatic Phase Transition Method)*. West Conshohocken, PA: ASTM International. www.astm.org.

ASTM D6450 (2021). *Standard Test Method for Flash Point by Continuously Closed Cup (CCCFP) Tester*. West Conshohocken, PA: ASTM International. www.astm.org.

ASTM D7042 (2021). *Standard Test Method for Dynamic Viscosity and Density of Liquids by Stabinger Viscometer (And the Calculation of Kinematic Viscsoity)*. West Conshohocken, PA: ASTM International. www.astm.org.

ASTM D7566 (2015). *Standard Specification for Aviation Turbine Fuel Containing Synthesized Hydrocarbons*. West Conshohocken, PA: ASTM International. www.astm.org.

Balster, L. M., Corporan, E., DeWitt, M. J., Edwards, T., Ervin, J. S., Graham, J. L., et al. (2008). Development of an Advanced, Thermally Stable, Coal-Based Jet Fuel. *Fuel Process. Technol.* 89, 364–378. doi:10.1016/j.fuproc.2007.11.018

Barker, J. A., and Henderson, D. (1967). Perturbation Theory and Equation of State for Fluids. II. A Successful Theory of Liquids. *J. Chem. Phys.* 47, 4714–4721. doi:10.1063/1.1701689

Bradley, J-C., and Andrew, L. (2014). *Open Melting point Dataset*. doi:10.6084/m9.figshare.1031638

Bream, R., Watkin, D., and Cowley, A. (2006). Acta Crystallographica Section. *Methylcyclopentane* E62, 1211–1212. doi:10.1107/S1600536806006003

Calcote, H. F., and Manos, D. M. (1983). Effect of Molecular Structure on Incipient Soot Formation. *Combust. Flame* 49, 289–304. doi:10.1016/0010-2180(83)90172-4

Catoire, L., and Naudet, V. (2004). A Unique Equation to Estimate Flashpoints of Selected Pure Liquids Application to the Correction of Probably Erroneous Flashpoint Values. *J. Phys. Chem. Ref. Data* 33, 1083–1111. doi:10.1063/1.1835321

Chapman, W. G., Gubbins, K. E., Jackson, G., and Radosz, M. (1989). SAFT: Equation-Of-State Solution Model for Associating Fluids. *Fluid Phase Equilib.* 52, 31–38. doi:10.1016/0378-3812(89)80308-5

Chen, F., Li, N., Li, S., Li, G., Wang, A., Cong, Y., et al. (2016). Synthesis of Jet Fuel Range Cycloalkanes with Diacetone Alcohol from Lignocellulose. *Green. Chem.* 18, 5751–5755. doi:10.1039/C6GC01497F

Chen, F., Li, N., Yang, X., Li, S., Li, G., Li, S., et al. (2016). Synthesis of High-Density Aviation Fuel with Cyclopentanol. *ACS. Sustain. Chem. Eng.* 4, 6160–6166. doi:10.1021/acssuschemeng.6b01678

Corporan, E., Edwards, T., Shafer, L., DeWitt, M. J., Klingshirn, C., Zabarnick, S., et al. (2011). Chemical, Thermal Stability, Seal Swell, and Emissions Studies of Alternative Jet Fuels. *Energy Fuels* 25, 955–966. doi:10.1021/ef101520v

Crossley, S. P., Alvarez, W. E., and Resasco, D. E. (2008). Novel Micropyrolysis index (MPI) to Estiamte the Sooting Tendency of Fuels. *Energy Fuels* 22, 2455–2464. doi:10.1021/ef800058y

Das, D. D., John, St. P., McEnally, C. S., Kim, S., and Pfefferle, L. D. (2018). Measuring and Predicting Sooting Tendencies of Oxygenates, Alkanes, Alkenes, Cycloalkanes, and Aromatics in a Unified Scale. *Combust. Flame* 190, 349–364. doi:10.1016/j.combustflame.2017.12.005

Defense Technical Information Center (2013). *Petroleum Quality Information System 2013 Annual Report*. Fort Belvoir: Diversified Enterprises.

Drotloff, H., and Moller, M. (1987). On the Phase Transition of Cycloalkanes. *Thermochim. Acta* 112, 57–62. doi:10.1016/0040-6031(87)88079-6

Graham, J. L., Rahmes, T. F., Kay, M. C., Belieres, J-P., Kinder, J. D., Millett, S. A., et al. (2011). Impact of Alternative Jet Fuel and Fuel Blends on Non-metallic Materials Used in Commercial Aircraft Fuel Systems. Federal Aviation Administration Report DOT/FAA/AEE/2014-10.

Graham, J. L., Striebich, R. C., Myers, K. J., Minus, D. K., and Harrison, W. E. (2006). Swelling of Nitrile Rubber by Selected Aromatics Blended in a Synthetic Jet Fuel. *Energy Fuels* 20, 759–765. doi:10.1021/ef050191x

Gross, J., and Sadowski, G. (2002). Application of the Perturbed-Chain SAFT Equation of State to Associating Systems. *Ind. Eng. Chem. Res.* 41, 5510–5515. doi:10.1021/ie010954d

Gunbas, D. D., Algi, F., Hokelek, T., Watson, W. H., and Balci, M. (2005). Functionalization of Saturated Hydrocarbons. High Temperature Bromination of Octahydropentalene Part 19. *Tetrahedron* 61, 11177–11183. doi:10.1016/j.tet.2005.09.019

Hansen, C. M. (1967). *The Three Dimensional Solubility Parameter and Solvent Diffusion Coefficient: Their Importance in Surface Coating Formulation*. Copenhagen: Danish Technical Press. Dissertation.

Hasha, J. J., and Huang, S. G. (1979). Self-diffusion and Viscosity of Methylcyclohexane in the Dense Liquid Region. *J. Chem. Phys.* 71, 3996–4000. doi:10.1063/1.438155

FUNDING

SUPPLEMENTARY MATERIAL

The Supplementary Material for this article can be found online at: https://www.frontiersin.org/articles/10.3389/fenrg.2021.771697/full#supplementary-material

Heyne, J. (2018). Down-selected molecules, Dayton. Available at: https://docs.google.com/spreadsheets/d/1fnPldO1z6zrLixZUBe01mccWayGJG5jBv17HXgZzLYI/edit#gid=1784110097 (Accessed September, 2018).

Heyne, J. S., Boehman, A. L., and Kirby, S. (2009). Autoignition Studies of Trans- and Cis-Decalin in an Ignition Quality Tester (IQT) and the Development of a High thermal Stability Unifuel/Single Battlefiel Fuel. *Energy Fuels* 23, 5879–5885. doi:10.1021/ef900715m

Holladay, J., Abdullah, Z., and Heyne, J. (2020). Sustainable Aviation Fuel: Review of Technical Pathways. Available at: https://www.energy.gov/sites/prod/files/2020/09/f78/beto-sust-aviation-fuel-sep-2020.pdf (accessed December 16, 2021). doi:10.2172/1660415

Hunt, R. A. (1953). Relation of Smoke point to Molecular Structure. *Ind. Eng. Chem.* 45, 602–606. doi:10.1021/ie50519a039

International Energy Outlook (2016). Transportation Sector Energy Consumption. Available at: https://www.eia.gov/outlooks/ieo/pdf/transportation.pdf (accessed July 12, 2021).

John, St. P., Kairys, P. W., Das, D. D., McEnally, C. S., Pfefferle, L. D., Robichaud, D. J., et al. (2017). A Quantitative Model for the Prediction of Sooting Tendency from Molecular Structure. *Energy Fuels* 31, 9983–9990. doi:10.1021/acs.energyfuels.7b00616

Kazakov, A. F., Muzy, C. D., Chirico, R., Diky, V., and Frenkel, M., NIST/TRC Web Thermo Tables-Professional Edition NIST Standard Reference Subscription Database 3, NIST/TRC Web Thermo Tables-Professional Edition NIST Standard Reference Subscription Database 3. 2002.

Kendhale, A. M., Gonnade, R., Rajamohanan, P. R., and Sanjayan, G. J. (2008). A Rigid bicyclo[3.3.0]octane (Octahydropentalene): a Heavily Constrained Novel Aliphatic Template for Molecular Self-Assembly. *Tetrahedron Lett.* 49, 3056–3059. doi:10.1016/j.tetlet.2008.03.062

Kirby, J., Geiselman, G. M., Yaegashi, J., Kim, J., Zhuang, X., Tran-Gyamfi, M. B., et al. (2021). Further Engineering of R. Toruloides for the Production of Terpenes from Lignocellulosic Biomass. *Biotechnol. Biofuels* 14, 101. doi:10.1186/s13068-021-01950-w

Kosir, S., Heyne, J., and Graham, J. (2020). A Machine Learning Framework for Drop-In Volume Swell Characteristics of Sustainable Aviation Fuel. *Fuel* 274, 117832. doi:10.1016/j.fuel.2020.117832

Lemaire, R., Lapalme, D., and Seers, P. (2015). Analysis of the Sooting Propensity of C-4 and C-5 Oxygenates: Comparison of Sooting Indexes Issued from Laser-Based Experiments and Group Additivity Approaches. *Combust. Flame* 162, 3140–3155. doi:10.1016/j.combustflame.2015.03.018

Lemaire, R., Le Corre, G., and Nakouri, M. (2021). Predicting the Propensity to Soot of Hydrocarbons and Oxygenated Molecules by Means of Structural Group Contribution Factors Derived from the Processing of Unified Sooting Indexes. *Fuel* 302, 121104. doi:10.1016/j.fuel.2021.121104

Li, H., Jiang, W., Liang, W., Huang, J., Mo, Y., Ding, Y., et al. (2014). Induced marine Fungus Chondrostereum Sp. As a Means of Producing New Sesquiterpenoids Chondrosterins I and J by Using Glycerol as the Carbon Source. *Mar. Drugs* 12, 167–175. doi:10.3390/md12010167

Li, K., Zhou, F., Liu, X., Ma, H., Deng, J., Xu, G., et al. (2020). Hydrodeoxygenation of Lignocellulose-Derived Oxygenates to Diesel or Jet Fuel Range Alkanes under Mild Conditions. *Catal. Sci. Technol.* 10, 1151–1160. doi:10.1039/C9CY02367D

Liu, Y., and Wilson, C. W. (2012). Investigation into the Impact of N-Decane, Decalin, and Isoparaffinic Solvent on Elastomeric Sealing Materials. *Adv. Mech. Eng.* 4, 127430. doi:10.1155/2012/127430

McEnally, C. S., and Pfefferle, L. D. (2007). Improved Sooting Tendency Measurements for Aromatic Hydrocarbons and Their Implications for Naphthalene Formation Pathways. *Combust. Flame* 148, 210–222. doi:10.1016/j.combustflame.2006.11.003

Milhet, M., Pauly, J., Coutinho, J. A. P., and Daridon, J. (2007). Solid-Liquid Equilibria under High-Pressure of Eight Pure N-Alkylcyclohexanes. *J. Chem. Eng. Data* 52, 1250–1254. doi:10.1021/je600575r

Montgomery, J. A., Jr., Frisch, M. J., Ochterski, J. W., and Petersson, G. A. (2000). A Complete Basis Set Model Chemistry. VII. Use of the Minimum Population Localization Method. *J. Chem. Phys.* 112, 6532–6542. doi:10.1063/1.481224

Muldoon, J. A., and Harvey, B. G. (2020). Bio-Based Cycloalkanes: The Missing Link to High-Performance Sustainable Jet Fuels. *ChemSusChem* 13, 5777–5807. doi:10.1002/cssc.202001641

Perez, A. G., Coquelet, C., Paricaud, P., and Chapoy, A. (2017). Comparative Study of Vapour-Liquid Equilibrium and Density Modeling of Mixtures Reltated to Carbon Capture and Storage with the SRK, PR, PC-SAFT and SAFT-VR Mie Equations of State for Industrial Uses. *Fluid Phase Equilib.* 440, 19–35. doi:10.1016/j.fluid.2017.02.018

Pokon, E. K., Liptak, M. D., Feldgus, S., and Shields, G. C. (2001). Comparison of CBS-QB3, CBS-APNO, and G3 Predictions of Gas Phase Deprotonation Data. *J. Phys. Chem. A.* 105, 10483–10487. doi:10.1021/jp012920p

Romanczyk, M., Ramirez Velasco, J. H., Xu, L., VozkaDissanayake, P. P., Dissanayake, P., Wehde, K. E., et al. (2019). The Capability of Organic Compounds to Swell Acrylonitrile Butadiene O-Rings and Their Effects on O-Ring Mechanical Properties. *Fuel* 238, 483–492. doi:10.1016/j.fuel.2018.10.103

Rosenkoetter, K. E., Kennedy, C. R., Chirik, P. J., and Harvey, B. G. (2019). [4+4]-Cycloaddition of Isoprene for the Production of High-Performance Bio-Based Jet Fuel. *Green. Chem.* 21, 5616–5623. doi:10.1039/C9GC02404B

Schalla, R. L., and McDonald, G. E. (1953). Variation in Smoking Tendency Among Hydrocarbons of Low Molecular Weight. *Ind. Eng. Chem.* 45, 1497–1500. doi:10.1021/ie50523a038

Sims, R. E. H., Creutzig, F., Cruz-Nunez, X., D'Agosto, M., Dimitriu, D., Meza, M. J. F., et al. (2014). in *Transport in Climate Change 2014: Mitigation of Climate Change. Contribution of Working Group III to the Fifth Assesment Report of the Intergovernmental Panel on Climate Change.* Editors P.-M. R. Edenhofer O., Y. Sokona, E. Farahani, S. Kadner, K. Seyboth, A. Adler, et al. (Cambridge, United Kingdom and New York, NY, USA: Cambridge University Press).

Sirjean, B., Glaude, P. A., Ruiz-Lopez, M. F., and Fournet, R. (2006). Detailed Kinetic Study of the Ring Opening of Cycloalkanes by CBS-QB3 Calculations. *J. Phys. Chem. A.* 110, 12693–12704. doi:10.1021/jp0651081

Wang, X., Liu, W., Xin, C., Zheng, Y., Cheng, Y., Sun, S., et al. (2016). Enhanced Limonene Production in Cyanobacteria Reveals Photosynthesis Limitations. *Proc. Natl. Acad. Sci.* 113, 14225–14230. doi:10.1073/pnas.1613340113

Wertheim, M. S. (1984). Fluids with Highly Directional Attractive Forces. II. Thermodynamic Perturbation Theory and Integral Equations. *J. Statist. Phys.* 35, 35–47. doi:10.1007/bf01017363

Wertheim, M. S. (1984). Fluids with Highly Directional Attractive Forces. I. Statistical Thermodynamics. *J. Statist. Phys.* 35, 19–34. doi:10.1007/bf01017362

Wertheim, M. S. (1986a). Fluids with Highly Directional Attractive Forces. I. Multiple Attraction Sites. *J. Statist. Phys.* 42, 459–476. doi:10.1007/bf01127721

Wertheim, M. S. (1986b). Fluids with Highly Directional Attractive Forces. IV. Equilibrium Polymerization. *J. Statist. Phys.* 42, 477–492. doi:10.1007/bf01127722

Woodrow, W. A. (1933). *Second World Petroleum Congr.* 2 Proc. 732.

Yang, J., Xin, Z., He, Q., Corscadden, K., and Niu, H. (2019). An Overview on Performance Characteristics of Bio-Jet Fuels. *Fuel* 237, 916–936. doi:10.1016/j.fuel.2018.10.079

Ysi database v2 (2021). Yield Sooting Index Database Volume 2: Sooting Tendencies of a Wide Range of Fuel Compounds on a Unified Scale. Available from: https://dataverse.harvard.edu/dataset/xhtml?persistentId=10.7910/DVN/7HGFT8 (Cited July 31, 2021).